BJR, 2025, **98**, 938–946
https://doi.org/10.1093/bjr/tqaf058
Advance access publication: 14 March 2025
Research Article

Splenial angle on axial T1 and fluid-attenuated inversion-recovery MRI images and idiopathic normal pressure hydrocephalus

Samantha Lee, MD[1], Robert Chen, MD[1,2,3], Sumeet Kumar, MD[2,3], Weiling Lee, MMRT[4], Huihua Li, PhD[3,5], Louis C.S. Tan, MD[3,6], Eng King Tan, MD[3,6], Nicole C.H. Keong, MD, MPhil[3,7], Ling Ling Chan, MD*[,1,2,3]

[1]Department of Neuroradiology, Singapore General Hospital, Singapore 169608, Singapore
[2]Department of Neuroradiology, National Neuroscience Institute, Singapore 308433, Singapore
[3]Duke-NUS Medical School, Singapore 169857, Singapore
[4]Department of Radiography, Singapore General Hospital, Singapore 169608, Singapore
[5]National Dental Centre, Singapore 168938, Singapore
[6]Department of Neurology, National Neuroscience Institute, Singapore 308433, Singapore
[7]Department of Neurosurgery, National Neuroscience Institute, Singapore 308433, Singapore

*Corresponding author: Ling Ling Chan, MD, Department of Neuroradiology, Singapore General Hospital, Outram Road, Singapore 169608, Singapore (chan.ling.ling@singhealth.com.sg)

Abstract

Objectives: The splenial angle (SA), measured on axial DTI colour fractional anisotropy MRI, outperformed the callosal angle (CA) in predicting idiopathic normal pressure hydrocephalus (NPH) patients from those with Alzheimer's dementia, Parkinson's disease (PD), and healthy controls (HC). We investigated its reliability and classification performance on more commonly acquired T1 magnetization-prepared rapid gradient-echo (MPRAGE) and fluid-attenuated inversion-recovery (FLAIR) images.

Methods: Splenial angle was measured on axial MPRAGE and FLAIR images in 57 subjects (19 NPH, PD and HC each) by 2 raters and compared across groups. Receiver operating characteristics (ROC) analysis was used to assess its classification performance, differentiating NPH from non-NPH groups, in comparison to the CA.

Results: Inter-rater reliability for SA was excellent (intraclass correlation coefficients ≥ 0.91). Splenial angle was effective in differentiating NPH from non-NPH patients on MPRAGE and FLAIR images ($P < .001$). Its ROC curves showed excellent performance classifying NPH from HC (Area under the curve [AUC] 1) and PD (AUC > 0.93) groups and were highly comparable to those for CA (1; 0.947). Angles wider than 60° and narrower than 45° robustly (100%) excluded and predicted NPH from HC, respectively. The narrower 45° cutoff yielded better sensitivity (84.2%-89.5%) in differentiating NPH from PD patients.

Conclusions: The SA on MPRAGE/FLAIR images showed excellent inter-rater reliability and classification performance predicting NPH from non-NPH groups, rivalling those of the CA.

Advances in knowledge: The SA on MPRAGE and FLAIR images is reproducible and shows excellent diagnostic performance, differentiating NPH from non-NPH groups, with potential to replace the CA in NPH screening given its accessibility on routine axial neuroimaging.

Keywords: normal pressure hydrocephalus; neurodegeneration; reproducibility; sensitivity and specificity; ROC curve.

Introduction

Idiopathic normal pressure hydrocephalus (NPH) is defined as a clinicopathological condition related to deranged cerebrospinal fluid (CSF) flow dynamics in the absence of secondary causes such as subarachnoid haemorrhage or meningitis.[1,2] It remains one of the most controversial neurological diseases, largely because its pathophysiology remains poorly understood.[2,3] Normal pressure hydrocephalus is widely believed to be underdiagnosed and under-reported. It is an entity of the elderly, and its prevalence increases with age, with 3.7% of people ≥65 years and up to 8.9% of those ≥80 years reported to be affected.[4,5] Patients classically experience an insidious onset of symptoms, inclusive of the triad of gait disorder, cognitive disturbance, and urinary incontinence. Clinically, gait dysfunction and a second cardinal symptom suffice for diagnosis.[6] These symptoms, however, are non-specific and often overlap with other common neurodegenerative disorders seen in the elderly, such as parkinsonism and dementia. Making an early and accurate diagnosis of NPH is paramount because gait abnormalities, dementia, and incontinence may be ameliorated or even cured by shunt surgery if detected within 2 years of symptom onset in selected patients.[6-8] On the other hand, symptoms may be irreversible if treatment is postponed.

Besides evaluation of gait, urodynamics and standardized neurocognitive tests as part of the NPH diagnostic workup, assessment of CSF drainage and flow also are useful for prognosticating patient response to surgical shunting.[1] The CSF tap test and prolonged external lumbar drainage simulate a patient's response to shunt surgery, while the CSF infusion test evaluates CSF outflow resistance, which is known to

Received: 28 February 2024; **Revised:** 13 January 2025; **Accepted:** 6 March 2025

increase in NPH.[9] However, these tests are invasive and may require short hospitalization for monitoring of response, besides carrying attendant risks such as infection, bleeding, or nerve injury. Hence, non-invasive neuroimaging techniques are important supplementary diagnostic tools prior to more invasive clinical workup.

Radiologically, ventriculomegaly in the absence of anatomical obstruction within the ventricular system is a key feature in NPH. This can be quantified with some specificity using the callosal angle (CA), and cut-off values had been reported, which facilitated patient selection for surgical shunting.[10] However, the CA is measured on coronal images and suffers from poor test-retest reproducibility.[11,12] Recently, the splenial angle (SA) was coined as an alternative to the CA, measured on the default axial plane and subtended at the posterior end of the corpus callosum. The SA was able to encapsulate the vulnerability of the posterior elements of the corpus callosum to ventriculomegalic stresses in idiopathic NPH, in comparison to generic ex vacuo ventriculomegaly in pathological neurodegeneration and physiological ageing, and showed morphologic changes post-shunting.[13,14] The test-retest reliability of the SA was excellent on DTI colour fractional anisotropy (FA) MRI when measured at the callosal-body level.[13] However, on T1 magnetizationprepared rapid gradient-echo (MPRAGE) images and measured at the level of the splenium, it demonstrated worst inter-rater reliability compared to the axial angle at the genu and coronal CAs at the anterior and posterior commissures.[14] The aim of this study was to evaluate the inter-rater reliability and classification performance of the SA for NPH, measured at the highest callosal-septal level on commonly acquired T1 MPRAGE and fluid-attenuated inversion-recovery (FLAIR) sequences in the axial plane. Secondarily, these findings were compared against those of the traditional CA.

Methods

Clinical

A total of 57 subjects were included in this study. Written informed consent for human research approved by our institutional ethics review board was obtained from each study participant. A flow chart of the study design and detailed subject inclusion and exclusion criteria are provided in Figure S1.

Nineteen NPH patients were recruited using a study protocol adapted from international guidelines,[6,15-17] as part of the NPH program at our tertiary referral center. Anonymized images of Parkinson's disease (PD) and healthy control (HC) subjects from existing case-control PD cohort database, age-, and sex-matched to the NPH cohort were included for comparison. The NPH patients were diagnosed with probable or possible NPH according to established criteria, based on clinical criteria (key symptoms, neuropsychological testing and CSF drainage) and ventriculomegaly (Evans index ≥ 0.30) not attributable to CSF obstruction or cerebral atrophy on neuroimaging.[6,15] To ensure a high confidence of NPH diagnosis, participants who did not meet these criteria were excluded.[16] The PD patients (including those with the postural instability and gait disorder subtype) were recruited from our movement disorder clinics,[18,19] where clinical diagnosis was made based on established criteria defined by the Advisory Council of the United States National Institute of Neurological Disorders and Stroke.[20] Patients with cognitive and/or musculoskeletal dysfunction, stroke, NPH, Parkinson-plus syndromes and secondary parkinsonism were excluded. The HC participants were healthy individuals from the population without neurological conditions. Background vascular risk factors and incidental mild cognitive impairment on basic screening were non-exclusionary for study subjects in this database.

MRI acquisition

All brain MRI scans were performed on 3-Tesla scanners using the following sequences: (1) three-dimensional (3D) T1-weighted high-resolution MPRAGE (coronal or sagittal acquisitions; $0.9 \times 0.9 \times 0.9$ mm^3; 1900/2.48) and (2) 2D FLAIR [axial acquisition parallel to the bi-commissural (AC-PC) line; voxel size $0.8 \times 0.8 \times 4$ mm^3; repetition time ms/echo time ms, 7700/134].

Image analysis

Splenial angle measurements were performed by 2 blinded independent raters: a neuroradiologist with more than 2 decades of experience and a radiology trainee with 1 year of experience. The 3D T1-weighted MPRAGE scans were reformatted into 1 mm axial/coronal images parallel/perpendicular to the central inter-commissural line through the AC-PC. No further image reformatting was needed for the directly acquired axial FLAIR images. The callosal angle on coronal T1 MPRAGE images was measured as previously described.[10-13]

For T1 MPRAGE and FLAIR images, the axial image containing the highest/most superior cut through the septum pellucidum, at or just below the callosal-septal interface landmark, is chosen for SA measurement (Figure 1). This slice is where the lateral ventricles last remain conjoined at the septum, and before their roofs are separated by the corpus callosal-body. Splenial angle is measured between the posteromedial margins of the lateral ventricles on this slice. In subjects with a patent cavum verghae, the 2 leaves of the septum pellucidum (cavum walls) are separated instead of being fused as one. The SA is still measured in the same manner (Figure 2).

Statistical analysis

Data analysis was performed using R 3.6.2 (https://www.r-project.org). Inter-rater reliability was assessed by the intraclass correlation coefficient (ICC) for all angle measurements. Further to the ICC results indicating excellent interrater reliability, angle measurements between raters were averaged for comparison across subject groups. Mean angles and 95% confidence intervals (CI) were reported. Analysis of Variance (ANOVA) was carried out to compare across NPH, PD, and HC groups. Receiver operating characteristic (ROC) curves were obtained to evaluate the sensitivity and specificity of the angles in predicting NPH from non-NPH groups.

Results

The NPH, PD, and HC participants were elderly (mean age 73.7 ± 6.36, 73.6 ± 5.74, and 72.3 ± 5.38, respectively), with 11 men and 8 women in each group. Inter-rater ICC for SA on T1 MPRAGE (0.96, 95% CI, 0.87-0.97) and FLAIR (0.91, 95% CI, 0.84-0.95) images were excellent and comparable to those for the CA (0.99, 95% CI, 0.98-0.99).

Mean SA on T1 MPRAGE and FLAIR images are detailed for NPH, PD, and HC groups in Table 1, in comparison to the CA. These were consistently widest in HC, followed by

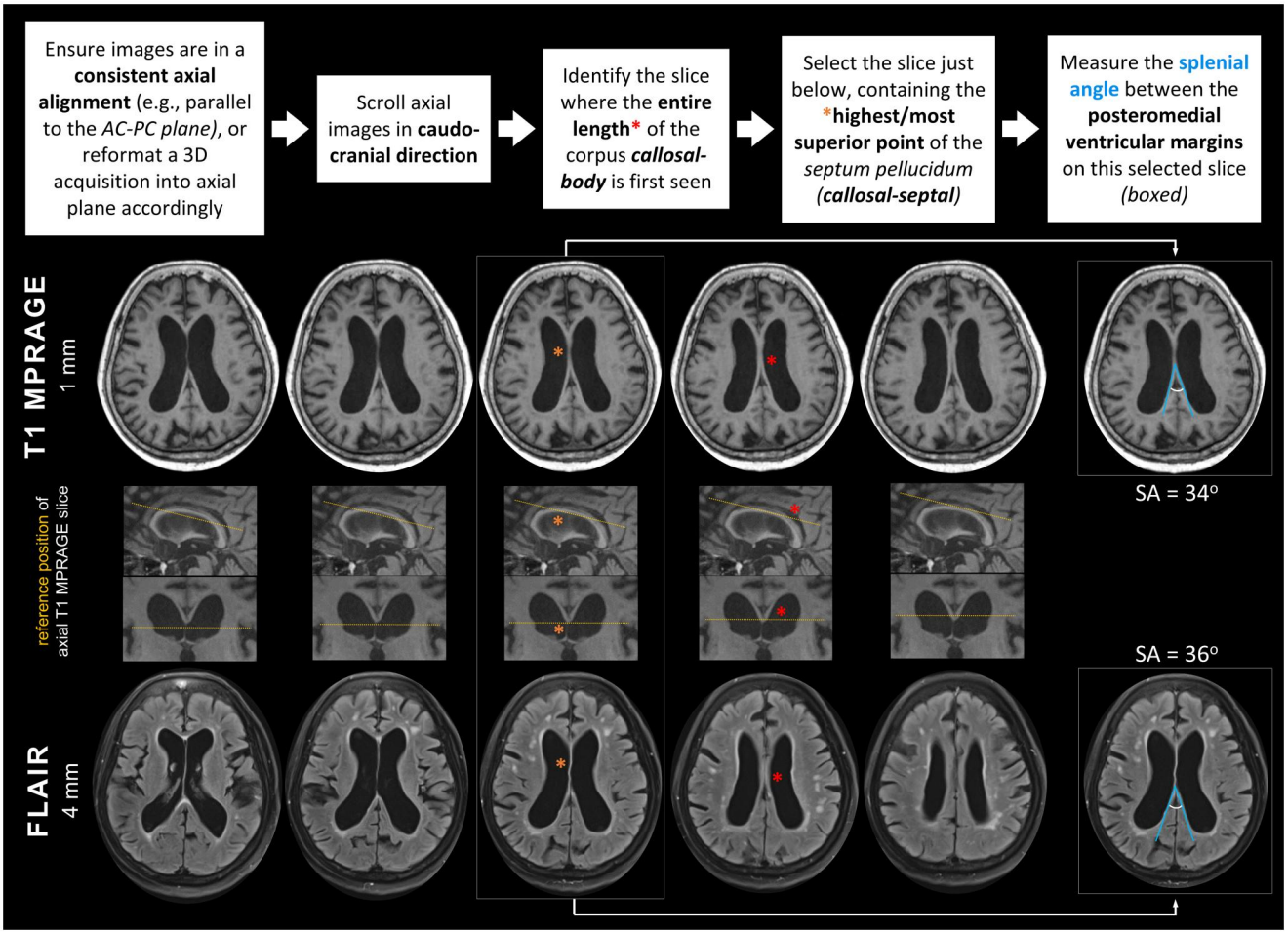

Figure 1. Splenial angle (SA) measurement on axial magnetization-prepared rapid gradient-echo (MPRAGE) and fluid-attenuated inversion-recovery (FLAIR) images. Schematic flow diagram (first row) and consecutive caudocranial (left to right) axial 1 mm MPRAGE (second row) and 4 mm FLAIR (fourth row) images in an 81-year-old female normal pressure hydrocephalus patient demonstrating slice selection (boxed in white) for splenial angle measurement (in blue) on the highest/most superior slice containing the septum pellucidum (callosal-septal level), as referenced by yellow dotted lines parallel to the anterior-posterior commissural line in the third row (upper inset) sagittal images. This axial slice is where the lateral ventricles are last conjoined at the septum before their roofs are separated by the corpus callosal-body as demonstrated on the third row (lower inset) coronal images. Note how angular narrowing between the posteromedial ventricular margins (SA in blue, right-most images) at the callosal-septal level effectively captures the greater compression on the posterior (splenial end) commissural fibres, compared to those at the genu (anterior end),[13] even on 4 mm-thick FLAIR images.

PD, and narrowest in NPH groups. All angles were effective in differentiating NPH from non-NPH groups ($P < .001$). Figure 3 shows the SA spread between raters and across groups for T1 MPRAGE and FLAIR images, with good distinction between NPH and HC groups. The majority of PD patients showed SA similar to those of HCs, albeit a minority had narrower SA overlapping those of NPH patients.

The ROC curves (Figure 4) showed that the SA was efficacious (Area under the curve [AUC] > 0.9) in differentiating NPH from HC and PD groups on T1 MPRAGE and FLAIR images, using cut-off thresholds chosen by the closest to the top-left corner of the ROC plots. Detailed sensitivity, specificity, negative, and positive predictive values at more clinically practical cut-offs of 45° and 60° are also provided in Table 2. Both SA and the traditional CA were equally superb (AUC 1.0) in discriminating NPH patients from HC. Classification performance of the SA (AUC 0.964) was highly comparable to the CA (AUC 0.947) in classifying NPH from PD patients using the thin T1 MPRAGE images, and that of SA using 4 mm FLAIR images was not worse (AUC 0.934) (Figure 4).

Discussion

The lateral ventricular ballooning in NPH deforms the corpus callosum, thinning and stretching it against the rigid interhemispheric dural falx. There is greater vulnerability of the posterior, splenial end of the commissural white matter tract to the mechanical compression. This is manifest in worse superomedial angular displacement of the corpus callosum, as quantified by the CA on a coronal section centred at the posterior commissure. The morphologically worse compression and distortion at the splenial/posterior end of the corpus callosum, compared to the genu/anterior end is most obvious on directionally-encoded colour FA images on DTI (Figure 5). Significantly greater colour distortion of the normally red-encoded transversally directed commissural corpus callosal fibre tracts is often seen in NPH patients, and worse affecting the splenial/posterior compared to the genu/anterior end at the callosal-body level. Hence, the SA was originally proposed for measurement on the axial slice though the corpus callosal-body, as this section optimally demonstrated the differential commissural fibre tract compression revealed on

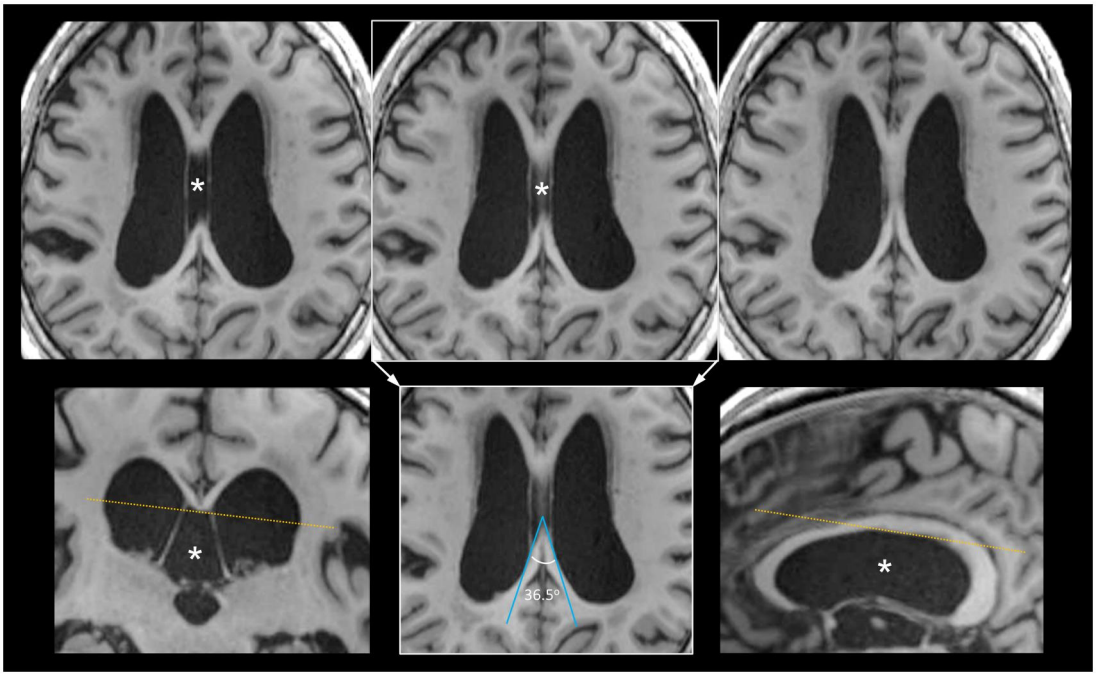

Figure 2. Patent cavum verghae and splenial angle (SA). Consecutive caudocranial (left to right) axial T1 magnetization-prepared rapid gradient-echo images (top row) from a 75-year-old male normal pressure hydrocephalus patient demonstrating a patent cavum verghae (asterisks). The slice (middle, boxed in white) just below the highest point of the callosal-septal interface, as depicted in yellow lines on reference coronal and sagittal images (bottom row, left, and right images, respectively), is selected for SA measurement. The vertex of the SA, subtended along the posteromedial margins of the lateral ventricles (bottom row, blue lines in middle image), projects into the cavum (asterisks).

Table 1. Mean splenial angle in HC, PD and NPH subjects measured at the highest callosal-septal junction on axial T1 MPRAGE and FLAIR images parallel to the AC-PC line, in comparison to the callosal angle.

Measurements	HC	PD	NPH	*P* value
Splenial angle (°)				
- T1 MPRAGE (callosal-septal)	75.34 ± 11.26	66.74 ± 16.35	30.37 ± 9.58	<.0001
- FLAIR (callosal-septal)	78.55 ± 10.17	65.61 ± 13.24	38.16 ± 8.73	<.0001
Callosal angle (°)	112.5 ± 8.28	105.2 ± 19.9	57.9 ± 15.3	<.0001

Abbreviations: AC, anterior commissure; FA, fractional anisotropy; FLAIR, fluid-attenuated inversion-recovery; HC, healthy control; MPRAGE, magnetization-prepared rapid gradient-echo; NPH, idiopathic normal pressure hydrocephalus; PC, posterior commissure; PD, Parkinson's disease.

DTI colour FA images.[13] In this study, we reconfigured the SA for measurement on T1 MPRAGE and FLAIR images on a section close to this anatomical level of interest (Figure 1). While directional connectivity information of the white matter tracts is not available on T1 MPRAGE and FLAIR images, the ependymal-CSF interfaces are crisp and sharp on these images. The angular differences between the limbs of the forceps minor (genu/anterior end) compared to that of the forceps major (splenial/posterior end) in NPH patients are harnessed, the latter as the SA (Figure 5). This is measured between the posteromedial lateral ventricular walls on these images at the callosal-septal level.

The SA measured on T1 MPRAGE and FLAIR images was effective in differentiating NPH from non-NPH groups (Table 1) and highly comparable to diagnostic performance of the traditional CA. A clinically practical SA cut-off of ≥60° excluded HC from NPH groups (sensitivity 100%, negative predictive value 100%), while an SA cut of ≤45° robustly predicted NPH from HC groups (specificity 100%, positive predictive value 100%) for both T1 MPRAGE and FLAIR images (partial volume effects on the 4 mm FLAIR notwithstanding). Differentiating NPH and PD groups was more challenging, and a narrower SA cut-off of ≤45° yielded better sensitivity (84.2%-89.5%) as a screening tool on both T1 MPRAGE and FLAIR images than an angle of 60°. Interestingly, our results and those from prior studies show that the SA that effectively discriminates NPH from non-NPH groups gets smaller as the section chosen for its measurement ascends from the splenium (71.1°),[14] through the callosal-septal (42°-59.5°) to the callosal-body (33.7°-43.9°)[13] levels. This progressively narrowing SA cutoff value suggests that the mechanical stresses on the corpus callosum worsen closer to the superior free edge of the interhemispheric falx.

The 1 mm-thin reformatted images of the 3D MPRAGE acquisition produced sharper lateral ventricular margins compared to the 4 mm thick FLAIR images, which produced mild blurring of the ventricular margins secondary to partial volume averaging of the curves of the convex ventricular roofs. However, this did not impede calliper placement for SA measurements (Figures 1 and 5). Instead, the thicker FLAIR sections helped remove potential between-rater variability in slice selection for measurement since there are limited FLAIR slices to choose from at the callosal-septal level compared to T1 MPRAGE images. Notably, inter-rater reliability of the SA on FLAIR remained excellent (ICC 0.91) and superior to that reported by Hattori et al,[14] using T1 MPRAGE images (0.86). The straight posteromedial ventricular walls directly abut at the callosal-septal level (Figure 1). At the splenium, they are separated by a curved "tip area,"[14] potentially contributing to inter-rater variability. These findings support the

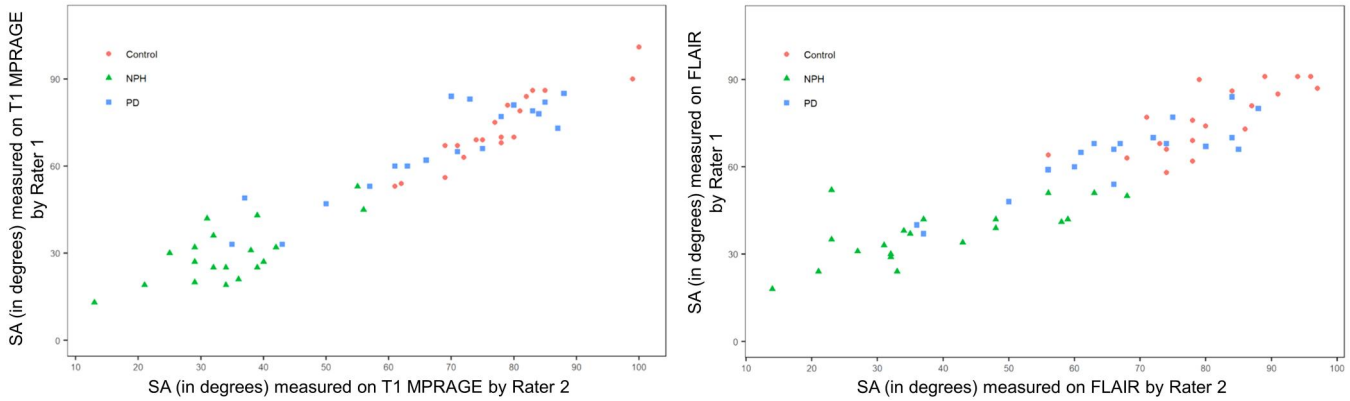

Figure 3. Scatterplots of splenial angles measured by raters 1 and 2 on T1 magnetization-prepared rapid gradient-echo and fluid-attenuated inversion-recovery images in patients with idiopathic normal pressure hydrocephalus, Parkinson's disease, and healthy controls.

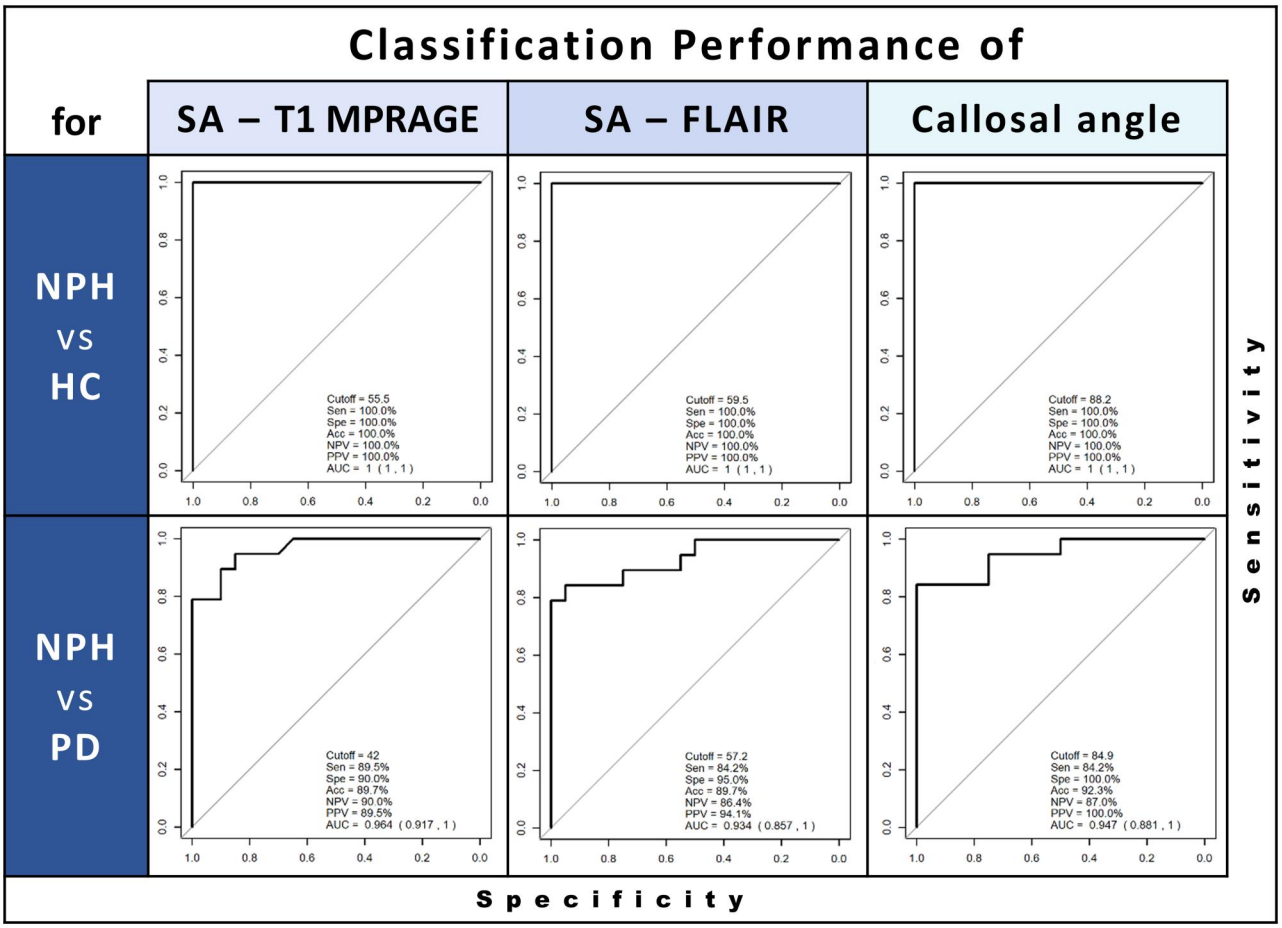

Figure 4. Performance metrics on receiver operating characteristics curves of the splenial angle on T1 magnetization-prepared rapid gradient-echo and fluid-attenuated inversion-recovery images and the callosal angle in differentiating between idiopathic normal pressure hydrocephalus, Parkinson's disease (PD), and healthy control groups.

callosal-septal SA on T1 MPRAGE/FLAIR images as a viable alternative to the CA and SA at the callosal-body/splenium.

Numerous qualitative and quantitative measurements and radiologic scales have been proposed to aid in the detection and diagnosis of NPH. Many require multiplanar image reformatting and/or offline volumetric evaluation, ranging from the "simplified" callosal angle on a defined coronal plane,[21] to the z-Evans index,[22] multiparametric Radscale,[23] and volumetric assessment of subarachnoid and ventricular spaces.[24] Many suffer from high test-retest variability, need for tedious multiplanar assessments, or the inconvenience of further image (eg, volumetric) postprocessing, hindering uniform incorporation in the clinics and across sites. Table 3 lists some of the classic cross-sectional NPH imaging features, related diagnostic biomarkers and their potential clinical utility.

Amongst these, the Evans index and CA[25] are the more accessible and familiar quantitative imaging biomarkers in

Table 2. Performance of SA in classification of NPH from HC and PD subjects using axial T1 MPRAGE and FLAIR Images.

Differentiating NPH from	SA (°) threshold	Specificity (%)	Sensitivity (%)	NPV (%)	PPV (%)
HC	**Using T1 MPRAGE images** (callosal-septal)				
	45	100.0	90.0	90.5	100.0
	60	89.5	100.0	100.0	90.9
Using FLAIR images (callosal-septal)					
	45	100.0	75.0	79.2	100.0
	60	94.7	100.0	100.0	95.2
PD	**Using T1 MPRAGE images** (callosal-septal)				
	45	90.0	84.2	85.7	88.9
	60	100.0	73.7	80.0	100.0
Using FLAIR images (callosal-septal)					
	45	70.0	89.5	87.5	73.9
	60	100.0	78.9	83.3	100.0

Abbreviations: FLAIR, fluid-attenuated inversion-recovery; HC, healthy control; MPRAGE, magnetization-prepared rapid gradient-echo; NPH, idiopathic normal pressure hydrocephalus; NPV, negative predictive value; PD, Parkinson's disease; PPV, positive predictive value; SA, splenial angle.

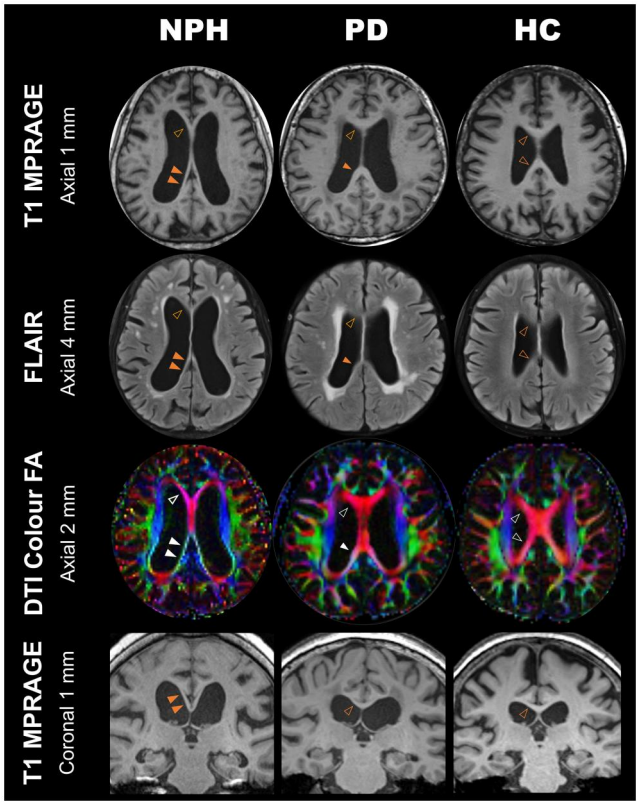

Figure 5. Greater vulnerability of the commissural fibres at the splenial/posterior end of the corpus callosum in idiopathic normal pressure hydrocephalus (NPH) depicted on T1 magnetization-prepared rapid gradient-echo (MPRAGE), fluid-attenuated inversion-recovery (FLAIR) and DTI colour fractional anisotropy (FA) images, and in contrast to Parkinson's disease (PD) and elderly healthy control (HC). More severe thinning and stretching of the splenial/posterior (double yellow arrowheads) corpus callosal fibres are seen against the ballooning ventriculomegaly compared to that anteriorly (open yellow arrowhead) in NPH (left column). This is most obvious on the DTI colour FA images (third row), where the normally red-encoded commissural fibres (see HC, right column) reveal significant discolouration (double white arrowheads) in the NPH.[13] This indicates their superomedial angular displacement and compression by the high rising ventricular roofs (fourth row, coronal images) in contrast to their more horizontal orientation in the HC (right column) and PD) (middle column). Note the narrower splenial angle in NPH (double arrowheads) subtended between the posteromedial ventricular walls, in comparison to that (single arrowheads) in PD and HC.

routine clinical practice. The Evans index, measured directly off axial images, is simple to calculate and able to quickly estimate the degree of ventriculomegaly. However, it is highly non-specific and can be abnormal in both neurodegenerative brain atrophy and non-neurodegenerative ventriculomegaly.[10,13,21] The CA is more specific than the Evans Index for diagnosing NPH,[10,25] and is suited for neuroradiological evaluation of patients with suspected NPH. However, the CA is known to produce significant variations if care is not undertaken to align the coronal image orthogonal to the bi-commissural plane before measurement.[11-13]

Differing coronal planes needed for radiological assessment of NPH and related neurological disorders hinder clinical implementation and radiological reporting. Alzheimer's disease may be a differential diagnosis for a patient suspected of NPH or even co-exist with NPH.[26] In this instance, assessment of medial temporal and entorhinal atrophy is performed on a coronal plane perpendicular to the long axis of the hippocampus or parallel to the posterior brainstem margin.[27,28] However, the tilt of this coronal plane differs from that for CA measurement (orthogonal to the AC-PC line). The high-resolution 3D T1 MPRAGE sequence has inherent multiplanar reconstruction capability and allows tweaking of the coronal reformats on the fly for standardized assessment at the clinical reporting workstation. Nonetheless, the need for 2 differentially angled coronal planes to accommodate quantitative evaluation for both NPH and Alzheimer's disease requires time for accurate image reformatting, exacerbates imaging archival needs, impedes reporting efficiency, and hampers accurate assessment of disease progression in longitudinal studies.[12] Besides, a 3D isotropic MPRAGE acquisition is non-standard in some radiology departments, compared to the more routine 2D axial images.

The SA combines the ease of the Evans index directly measured off an axial image with the specificity of the CA measured off the orthogonal coronal plane. This has wide scoping potential for convenient radiological implementation because the axial plane is the most commonly acquired in cross-sectional imaging and most familiar to the multidisciplinary team in the care of NPH patients. Hence, even if axial reformatting is needed from a non-axial 3D T1 MPRAGE acquisition, less time is expended training technologists, and the additional step to perform accurate coronal reformatting

Table 3. Classic imaging features of NPH, related imaging biomarkers and their significance.

Classic NPH imaging features and cross-sectional imaging biomarker					Significance
Lateral ventricular dilatation	**Linear**	**Axial** (∥ AC-PC line or otherwise)	Latero-Lateral	**Evans Index** (EI) = (a)/(b) ratio, where: (a) maximum frontal horn Ø (FHD) (b) maximum inner diameter of the skull on the same slice	EI >0.3: part of NPH diagnostic criteria in both international and Japanese NPH Guidelines [1,6]
		Coronal (⊥ AC-PC line)	Caudo-Cranial Vertical z-axis	**z-Evans Index** (zEI) = (a)/(b) ratio, where: (a) maximum frontal horn vertical Ø *at foramen of Monro* (b) maximum supratentorial intracranial Ø = bone-to-bone Ø on mid-sagittal section	zEI > 0.42[22]: • superior to EI for NPH Δ • 1.5× higher chance of CSF tap-positive response; AUC 0.76 predicting tap-positive versus tap-negative groups
	Angular	**Coronal** Caudo-Cranial	⊥ AC-PC line	**Callosal angle** (CA) = ∡ between superomedial ventricular walls *at PC*	CA • <90° discriminates NPH from AD and HC (accuracy 93%)[1,10] • <63° showed best accuracy (highest Youden's index, 0.33) predicting NPH shunt responders[10]
			∥ posterior brainstem margin/ fourth ventricular floor	**Simplified Callosal Angle** (sCA) = ∡ between superomedial ventricular walls *at corpus callosum midpoint*	sCA <123° accurately discriminated NPH from DLB/AD (AUC 0.99) [21]
		Axial Latero-Lateral (∥ AC-PC line)		**Splenial angle** (SA) and variations = ∡ between (a) limbs of forceps major *at callosal-body level* on **DTI FA images**[13] (b) posteromedial ventricular walls *at highest callosal-septal interface* [this study] and *callosal splenium level*[14] on **T1 MPRAGE/FLAIR images**	(a) Callosal-body SA predicts NPH from PD, AD and HC (AUC > 0.98) [13] (b) Callosal-septal SA predicts NPH from PD, HC (AUC ≥0.934) [our study]: • <45° predicts NPH • >60° excludes NPH
Disproportionate subarachnoid spaces	**Visual rating**	**Coronal** Caudo-Cranial		Various semiquantitative scales are used to identify/grade elements[23,30,31] of the **disproportionately enlarged subarachnoid space hydrocephalus (DESH) pattern**[1,15] and as revealed by CSF volumetric analysis,[22,24] including (a) disproportionality between the following: (b) Sylvian fissure enlargement (c) narrowing of parasagittal-superior convexity subarachnoid spaces	Among NPH patients[1]: • DESH pattern seen in 64% • non-DESH pattern in 36%. DESH score • *at PC (⊥ AC-PC line)* reliably differentiates NPH from HC (AUC 0.964)[30] • high scores (>6) predict positive response to shunt surgery[31]

Abbreviations: AC, anterior commissure; AD, Alzheimer's disease; DLB, dementia with Lewy bodies; HC, healthy controls; NPH, idiopathic normal pressure hydrocephalus; PD, Parkinson's disease; PC, posterior commissure; positive predictive value ; ∥, parallel; ⊥, perpendicular; Ø, diameter; ∡, angle; Δ, diagnosis.

for CA measurement is effectively obviated. The axial callosal-body SA on DTI colour FA images has been shown to outperform the Evans index and CA in differentiating NPH from non-NPH groups.[13] In our study, we demonstrated its effective translation into the callosal-septal SA on axial FLAIR/T1 MPRAGE with excellent inter-rater reliability and diagnostic performance discriminating NPH from non-NPH groups. More importantly, these results are highly comparable to those of the CA, suggesting that the SA could potentially replace/supplement the latter in NPH evaluation.

We did not include a dementia group for callosal-septal SA measurement on T1 MPRAGE and FLAIR images because previous studies already showed that SAs in patients with Alzheimer's disease lie within the angular ranges of HC and PD groups, and these groups were already included in the current evaluation.[13,14] In addition, the thrust of this study was to refashion the axial SA for consistent measurement on FLAIR and T1 MPRAGE images, so omission of the Alzheimer's disease group is unlikely to impact our findings. Hattori et al[14] made angular measurements between the posteromedial ventricular margins at the splenium level in patients with a wide range of clinical neurological diagnoses. They also found a wider range of angles in PD patients with/without cognitive dysfunction compared to Alzheimer's disease patients. In their study, PD patients with dementia had the narrowest angles after the NPH group, compared to wider angles similar to HC in PD patients without dementia. In addition, the authors showed that only axial angular measurement at the splenium showed a correlation with gait and cognitive scores compared to a host of hydrocephalus parameters, including the CA. Notably, the simplified CA[21] is technically measured at the same level as our callosal-septal SA (Table 3). These further point to the potential clinical value of an axial SA measured at this level.

Further multi-center evaluation of the SA on axial images at the callosal-body, highest callosal-septal, or callosal-splenium levels and in diverse neurological clinical conditions, with correlation to clinical markers, will help validate its clinical robustness. Similarly, further evaluation of SA changes in bigger cohorts of NPH patients before and after surgical intervention on axial FLAIR, T1 MPRAGE and DTI colour FA images will be useful in assessing their utility in predicting and monitoring response to surgical shunting.[13,14,29] Future studies could evaluate the SA on axial head CT images since this is the most prevalent and accessible neuroimaging screening modality in radiology and would make the SA more widely applicable in MRI-scarce centres.

In conclusion, we showed that the SA measured on axial T1 MPRAGE and FLAIR images is reproducible and effective in differentiating NPH ventriculomegaly from PD and normal aging. Callosal-septal SA $>60°$ and $<45°$ robustly excluded and predicted NPH from HC, respectively, while a narrower 45° cutoff yielded better sensitivity in the differentiating NPH from the more heterogenous PD group. Accessibility of the SA on axial routine neuroimaging would aid convenient identification and triaging of NPH patients for more invasive diagnostic investigations and suitability evaluation for symptom-reversing shunt surgery.

Supplementary material

Supplementary material is available at *BJR* online.

Funding

This study has received funding from the National Medical Research Council, Singapore: (a) NMRC/TA/0024/2013, (b) NMRC/TCR14/012, (c) NMRC/CSI/0006/2006, (d) NMRC/CSASI/0008/2020.

Conflicts of interest

None declared.

References

1. Nakajima M, Yamada S, Miyajima M, et al.; Research Committee of Idiopathic Normal Pressure Hydrocephalus. Guidelines for management of idiopathic normal pressure hydrocephalus (third edition): endorsed by the Japanese society of normal pressure hydrocephalus. *Neurol Med Chir (Tokyo)*. 2021;61:63-97. https://doi.org/10.2176/nmc.st.2020-0292
2. Nassar BR, Lippa CF. Idiopathic normal pressure hydrocephalus: a review for general practitioners. *Gerontol Geriatr Med*. 2016;2:2333721416643702. https://doi.org/10.1177/2333721416643702
3. Hakim S, Adams RD. The special clinical problem of symptomatic hydrocephalus with normal cerebrospinal fluid pressure. Observations on cerebrospinal fluid hydrodynamics. *J Neurol Sci*. 1965;2:307-327. https://doi.org/10.1016/0022-510x(65)90016-x
4. Andersson J, Rosell M, Kockum K, Lilja-Lund O, Söderström L, Laurell K. Prevalence of idiopathic normal pressure hydrocephalus: a prospective, population-based study. *PLoS One*. 2019;14:e0217705. https://doi.org/10.1371/journal.pone.0217705
5. Jaraj D, Rabiei K, Marlow T, Jensen C, Skoog I, Wikkelsø C. Prevalence of idiopathic normal-pressure hydrocephalus. *Neurology*. 2014;82:1449-1454. https://doi.org/10.1212/WNL.0000000000000342
6. Relkin N, Marmarou A, Klinge P, Bergsneider M, Black PM. Diagnosing idiopathic normal-pressure hydrocephalus. *Neurosurgery*. 2005;57:S4-S16. https://doi.org/10.1227/01.neu.0000168185.29659.c5
7. Wada T, Kazui H, Yamamoto D, et al. Reversibility of brain morphology after shunt operations and preoperative clinical symptoms in patients with idiopathic normal pressure hydrocephalus. *Psychogeriatrics*. 2013;13:41-48. https://doi.org/10.1111/psyg.12001
8. Shaw R, Mahant N, Jacobson E, Owler B. A Review of clinical outcomes for gait and other variables in the surgical treatment of idiopathic normal pressure hydrocephalus. *Mov Disord Clin Pract*. 2016;3:331-341. https://doi.org/10.1002/mdc3.12335
9. Williams MA, Malm J. Diagnosis and treatment of idiopathic normal pressure hydrocephalus. *Continuum (Minneap Minn)*. 2016;22:579-599. https://doi.org/10.1212/CON.0000000000000305
10. Virhammar J, Laurell K, Cesarini KG, Larsson EM. The callosal angle measured on MRI as a predictor of outcome in idiopathic normal-pressure hydrocephalus. *J Neurosurg*. 2014;120:178-184. https://doi.org/10.3171/2013.8.JNS13575
11. Ryska P, Slezak O, Eklund A, Salzer J, Malm J, Zizka J. Variability of normal pressure hydrocephalus imaging biomarkers with respect to section plane angulation: how wrong a radiologist can be? *AJNR Am J Neuroradiol*. 2021;42:1201-1207. https://doi.org/10.3174/ajnr.A7095
12. Lee W, Lee AJY, Li H, et al. Callosal angle in idiopathic normal pressure hydrocephalus: small angular malrotations of the coronal plane affect measurement reliability. *Neuroradiology*. 2021;63:1659-1667. https://doi.org/10.1007/s00234-021-02658-2
13. Chan LL, Chen R, Li H, et al. The splenial angle: a novel radiological index for idiopathic normal pressure hydrocephalus. *Eur Radiol*. 2021;31:9086-9097. https://doi.org/10.1007/s00330-021-07871-4

14. Hattori T, Ohara M, Yuasa T, et al. Correlation of callosal angle at the splenium with gait and cognition in normal pressure hydrocephalus. *J Neurosurg*. 2023;139:481-491. https://doi.org/10.3171/2022.12.JNS221825
15. Mori E, Ishikawa M, Kato T, et al.; Japanese Society of Normal Pressure Hydrocephalus. Guidelines for management of idiopathic normal pressure hydrocephalus: second edition. *Neurol Med Chir (Tokyo)*. 2012;52:775-809. https://doi.org/10.2176/nmc.52.775
16. Lock C, Kwok J, Kumar S, et al. DTI profiles for rapid description of cohorts at the clinical-research interface. *Front Med (Lausanne)*. 2019;5:357. https://doi.org/10.3389/fmed.2018.00357
17. Marmarou A, Black P, Bergsneider M, Klinge P, Relkin N; International NPH Consultant Group. Guidelines for management of idiopathic normal pressure hydrocephalus: progress to date. *Acta Neurochir Suppl*. 2005;95:237-240. https://doi.org/10.1007/3-211-32318-x_48
18. Chan LL, Ng KM, Rumpel H, Fook-Chong S, Li HH, Tan EK. Transcallosal diffusion tensor abnormalities in predominant gait disorder parkinsonism. *Parkinsonism Relat Disord*. 2014;20:53-59. https://doi.org/10.1016/j.parkreldis.2013.09.017
19. Huang X, Ng SY, Chia NS, et al. Serum uric acid level and its association with motor subtypes and non-motor symptoms in early Parkinson's disease: PALS study. *Parkinsonism Relat Disord*. 2018;55:50-54. https://doi.org/10.1016/j.parkreldis.2018.05.010
20. Gelb DJ, Oliver E, Gilman S. Diagnostic criteria for Parkinson disease. *Arch Neurol*. 1999;56:33-39. https://doi.org/10.1001/archneur.56.1.33
21. Cagnin A, Simioni M, Tagliapietra M, et al. A simplified callosal angle measure best differentiates idiopathic-normal pressure hydrocephalus from neurodegenerative dementia. *J Alzheimers Dis*. 2015;46:1033-1038. https://doi.org/10.3233/JAD-150107
22. Yamada S, Ishikawa M, Yamamoto K. Optimal diagnostic indices for idiopathic normal pressure hydrocephalus based on the 3D quantitative volumetric analysis for the cerebral ventricle and subarachnoid space. *AJNR Am J Neuroradiol*. 2015;36:2262-2269. https://doi.org/10.3174/ajnr.A4440
23. Kockum K, Lilja-Lund O, Larsson EM, et al. The idiopathic normal-pressure hydrocephalus Radscale: a radiological scale for structured evaluation. *Eur J Neurol*. 2018;25:569-576. https://doi.org/10.1111/ene.13555
24. Yamada S, Ishikawa M, Yamamoto K. Fluid distribution pattern in adult-onset congenital, idiopathic, and secondary normal-pressure hydrocephalus: implications for clinical care. *Front Neurol*. 2017;8:583. https://doi.org/10.3389/fneur.2017.00583
25. Miskin N, Patel H, Franceschi AM, et al.; Alzheimer's Disease Neuroimaging Initiative. Diagnosis of normal-pressure hydrocephalus: use of traditional measures in the era of volumetric MR imaging. *Radiology*. 2017;285:197-205. https://doi.org/10.1148/radiol.2017161216
26. Kiefer M, Unterberg A. The differential diagnosis and treatment of normal-pressure hydrocephalus. *Dtsch Arztebl Int*. 2012;109:15-25; quiz 26. https://doi.org/10.3238/arztebl.2012.0015
27. Scheltens P, Leys D, Barkhof F, et al. Atrophy of medial temporal lobes on MRI in "probable" Alzheimer's disease and normal ageing: diagnostic value and neuropsychological correlates. *J Neurol Neurosurg Psychiatry*. 1992;55:967-972. https://doi.org/10.1136/jnnp.55.10.967
28. Enkirch SJ, Traschütz A, Müller A, et al. The ERICA score: an MR imaging-based visual scoring system for the assessment of entorhinal cortex atrophy in Alzheimer disease. *Radiology*. 2018;288:226-333. https://doi.org/10.1148/radiol.2018171888
29. Virhammar J, Laurell K, Cesarini KG, Larsson EM. Increase in callosal angle and decrease in ventricular volume after shunt surgery in patients with idiopathic normal pressure hydrocephalus. *J Neurosurg*. 2019;130:130-135. https://doi.org/10.3171/2017.8.JNS17547
30. Ryska P, Slezak O, Eklund A, Malm J, Salzer J, Zizka J. Radiological markers of idiopathic normal pressure hydrocephalus: relative comparison of their diagnostic performance. *J Neurol Sci*. 2020;408:116581. https://doi.org/10.1016/j.jns.2019.116581
31. Shinoda N, Hirai O, Hori S, et al. Utility of MRI-based disproportionately enlarged subarachnoid space hydrocephalus scoring for predicting prognosis after surgery for idiopathic normal pressure hydrocephalus: clinical research. *J Neurosurg*. 2017;127:1436-1442. https://doi.org/10.3171/2016.9.JNS161080

British Journal of Radiology, 2025, 98, 938–946
https://doi.org/10.1093/bjr/tqaf058
Research Article